WPPFC-CPR(18) 18900

J Oelmann et al.

Depth resolved analysis of hydrogen content in W7-X tiles using Laser-Induced Ablation-Quadrupole Mass Spectrometry (LIA-QMS)

Preprint of Paper to be submitted for publication in Proceeding of 23rd International Conference on Plasma Surface Interactions in Controlled Fusion Devices (PSI-23)

This work has been carried out within the framework of the EUROfusion Consortium and has received funding from the Euratom research and training programme 2014-2018 under grant agreement No 633053. The views and opinions expressed herein do not necessarily reflect those of the European Commission.

Depth resolved analysis of hydrogen in W7–X graphite components using Laser–Induced Ablation–Quadrupole Mass Spectrometry (LIA–QMS)

Jannis Oelmann[a,*], Cong Li[a,b], Sebastijan Brezinsek[a], Marcin Rasinski[a], Chandra Prakash Dhard[c], Thomas Sunn Pedersen[c], Ralf König[c], Victoria Winters[d], Christian Linsmeier[a], the W7–X Team[c]

[a] *Forschungszentrum Jülich GmbH, Institut für Energie- und Klimaforschung – Plasmaphysik, Partner of the Trilateral Euregio Cluster (TEC), 52425 Jülich, Germany*

[b] *Key Laboratory of Materials Modification by Laser, Ion and Electron Beams, Chinese Ministry of Education, School of Physics, Dalian University of Technology, 116024 Dalian, PR China*

[c] *Max-Planck–Institut für Plasmaphysik, 17491 Greifswald, Germany*

[d] *University of Wisconsin –Madison, Department of Engineering Physics, Madison, WI, USA*

Abstract

A in–depth understanding of the plasma–wall interaction processes in fusion devices like Wendelstein 7–X is necessary for an efficient plasma operation and a long lifetime of the plasma–facing components.
In this work we present an approach employing residual gas analysis after picosecond laser–induced ablation (ps LIA–QMS) of graphite limiter tiles, exposed in the first plasma operational phase of Wendelstein 7–X, for depth–resolved and quantitative hydrogen content analysis. A series of poloidal and toroidal locations are analyzed at three of the five limiters, showing up to $2.3 \cdot 10^{22}$ hydrogen atoms/m^2 in net–deposition areas after a total plasma exposure of about 311 s in mixed hydrogen and helium operation. In the erosion zone, shallow implantation of hydrogen has been observed of which the fuel content depend on the limiter temperature during plasma operation. The hydrogen content spans between (1.1 and 3.7) $\cdot 10^{21}$ atoms/m^2 in the net–erosion areas. Moreover, oxygen has been analyzed and its appearance in both the implantation and deposition zone was verified. Results are compared to scanning electron microscopy, therdesorption spectrometry and to simultaneously performed laser–induced breakdown spectroscopy (LIBS) measurements.

Keywords: Laser–induced ablation, Quadrupole mass spectrometry, Laser–induced breakdown spectroscopy, Graphite plasma–facing components, Wendelstein 7–X, Limiter

1. Introduction

Monitoring plasma–wall interaction processes like erosion, redeposition, retention and outgassing in fusion devices like Wendelstein 7–X (W7–X) is essential for the lifetime of the first wall as well as for a better understanding of the fuel (hydrogen) retention[1, 2, 3]. This is especially important for long–time discharges of up to 1800 s in the next W7–X operation phases [4, 5] and for future fusion reactors operating with tritium, where a sustainable fuel cycle is required and a inventory limit for tritium will be present[6]. Using laser–based methods like Laser–Induced Breakdown Spectroscopy (LIBS), in–situ as well as ex–situ analysis can be performed preparation free[7, 8]. Still, the plasma formation and its characteristic light emission are non–equilibrium processes, which impedes quantitative analysis of unknown material compositions, although Calibration–Free LIBS (CF–LIBS) analysis improved[9, 10].
Most commonly used quantitative analysis methods like Nuclear Reaction Analysis (NRA) cannot give information about hydrogen, need detailed information about the sample composition (e.g. Secondary Ion Mass Spectrometry) or have no or poor depth resolution (e.g. Thermal Desorption Spectrometry (TDS)).
Post mortem analysis of graphite limiter tiles from the initial operational phase of W7–X in limiter configuration (OP 1.1)[11] have been performed recently: Scanning electron microscopy (SEM) with Focused Ion Beam (FIB) and Energy Dispersive X–ray (EDX) analysis shows different surface structures, owing to local re–deposition (rough) and background deposition (smooth)[12]. LIBS analysis in toroidal direction of the limiter showed a higher hydrogen content at the outer parts of the limiter[13] as eroded carbon from the central part is re–deposited in this regions with co–depostion of oxygen and hydrogen.
We present additional information on these limiter tiles using the technique of picosecond Laser–Induced Ablation–Quadrupole Mass Spectrometry (LIA–QMS)[14]. It is one of a limited number of post–mortem analysis diagnostics which allows quantitative and depth–resolved information of the hydrogen content in graphite components.

*Corresponding author.
Email address: j.oelmann@fz-juelich.de (Jannis Oelmann)

As a residual gas analysis, only volatile sample components can be detected, which is why LIBS is performed simultaneously in one setup under different observation angles. This contribution consists of five sections: The introduction is followed by information concerning samples from W7–X and plasma exposure conditions (section 2). The combined setup for LIBS and LIA–QMS as well as details to these techniques are presented in section 3. Limiter tile analysis results comparing three different limiters in poloidal and toroidal direction and a discussion are shown in section 4. Finally, a conclusion is given in section 5.

2. Samples

Figure 1: Photo of limiter modules 5 to 1 (left to right), each containing nine tiles. Analyzed tiles are marked in red. On limiter 4 a simulation of the heat flux (EMC3–EIRENE code[11]) owing to electron and ion impact is overlayed.

In operation phase 1.1, five equivalent graphite limiter were installed in W7–X. They were exposed to helium and hydrogen plasmas with a total exposure time of about 311 s [15]. Each limiter consists of nine tiles. The analyzed positions with their labels are shown in Fig. 1. The overlay shows a simulation of EMC3–EIRENE code for the heat flux in a standard magnetic configuration of W7–X hydrogen plasma. Two stripes of high heat fluxes in poloidal direction are observed on the limiter. Its maxima are observed on tiles 3 and 6 for the left and right side of the limiter respectively. The simulation predicts an asymmetry in toroidal direction of one tile and an asymmetry on one limiter in poloidal direction due to the imposed magnetic field structure with different connection lengths[11]. Here, we use the hydrogen content in the tiles to study if the asymmetries in the impinging ion and heat flux can be observed by post–mortem analysis techniques. Additionally, a comparison of limiter 1,2 and 4 is shown, as limiter 1 was positioned slightly deeper into the plasma and achieved higher heat loads[11].

3. Experimental Setup

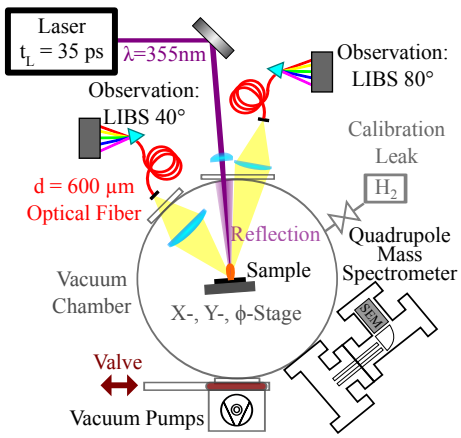

Figure 2: Schematic overview of the setup: Single picosecond laser pulses are used to succesive ablate a sample in a vacuum chamber. A combination of laser induced breakdown spectroscopy and residual gas analysis is used to measure the sample's composition. A valve to the vacuum pumps is closed for the residual gas analysis and for sprectrometrical calibration (based on [14]).

The experimental setup for picosecond laser–induced ablation using a Nd:YVO_4 laser by *EKSPLA* is shown in Fig. 2. The samples are mounted on a x–, y–, ϕ–stage in a vacuum chamber with a base pressure of $p_0 = 1 \cdot 10^{-7}$ mbar and excited perpendicular to the surface. The limiter tiles are cut into 7 pieces to reduce a change of the excitation fluency caused by its curved surface. This results in an excitation angle of 90°±5°. An increase of the laser spot size is neglected. To perform residual gas analysis after laser–induced ablation (LIA–QMS), a valve to the vacuum pumps can be closed. Simultaneously, LIBS is performed with observation angles of 40° and 80°. The laser parameter and settings are shown in Tab. 1.

Table 1: Overview of the laser parameter and settings used for the analysis of W7–X graphite limiter tiles.

Laser wavelength:	λ_L	$= 355\,\mathrm{nm}$
Pulse duration:	t_L	$= 35\,\mathrm{ps}$
Pulse energy:	E_L	$= 25\,\mathrm{mJ}$
Spot diameter at sample:	d_L	$= 700\,\mu\mathrm{m}$
Average laser fluency:	F_L	$= 6.5\,\mathrm{J/cm^2}$

3.1. Diagnostics

With the setup shown in Fig. 2, LIA–QMS and LIBS are be performed simultaneously to get sample composition information from characteristic line radiation (LIBS) with additional quantitative information of volatile species (LIA–QMS). Using the laser parameter shown in Tab. 1, a depth resolution of ≈ 100 nm and a lateral resolution of up to 2 mm is achieved.
In addition, the samples were analyzed with SEM, FIB and EDX techniques. Details can be found in [12]. Also, TDS

was performed with surface cuts ($l \cdot w \cdot h = (8 \cdot 8 \cdot 4)\,\mathrm{mm}^3$) of the limiter tiles, assuming there was no interaction of hydrogen in the material in the depth beyond 1 mm. TDS is used as independent measure of the quantitative hydrogen content, without any depth resolution, but as integral measure.

3.1.1. LIA–QMS

Laser–induced ablation–quadrupole mass spectrometry is a relative novel method to determine volatile sample components. After closing a valve to the vacuum pumps, the sample is excited with a high energetic picosecond laser pulse. The partial pressure of removed material in gas phase up to 100 u/e is detected in quasi–equilibrium[1] with a quadrupole mass spectrometer. Details to the measurement technique can be found in [14]. For all measurements shown in this publication, a constant measurement signal, which is observed after 15 subsequent laser pulses on one sample position is subtracted as background signal. Consequently, only the plasma–induced signal rises close to the surface are analyzed, whereas intrinsic components and parasitic signals from interaction of the laser radiation with the chamber wall are subtracted.

3.1.2. LIBS

For laser–induced breakdown spectroscopy, two spectrometers with observation angles of 40° and 80° to the sample's surface are used: One Ocean Optics, *HR2000* USB spectrometer (wavelength range from 350 nm to 800 nm) and a high resolution spectrometer with a wavelength range in the order of 10 nm. More details to the LIBS setup and its analysis of the limiter tiles can be found in [13].

4. Results and discussion

The surface composition of different positions on the graphite limiters is analyzed. Fig. 3 shows a photo of limiter 4 – tile 3 with labeling for toroidal and poloidal scanning direction.

4.1. Toroidal: Limiter 4 – tile 3 and tile 6

A scan over the limiter tiles in toroidal direction with a lateral resolution up to 2 mm is performed. The integrated signal of ten successive laser–induced ablations, giving a total ablation depth of 1 μm is shown in Fig. 4 for tile 3 and 6. Regarding tile 3, the hydrogen content shows a symmetry for the left and right part with two maxima on each side of the limiter. The maximum at the outside of the right side ($x \approx 70$ mm) of the tile is slightly broader than the on the left side, which is attributed to the shape of the limiter.

[1] The term *quasi–equilibrium* us used to describe a constant partial pressure, caused by laser–induced sample abltion, which is superposed with a linear rise of the background signal, caused by outgassing of the vacuum chamber wall.

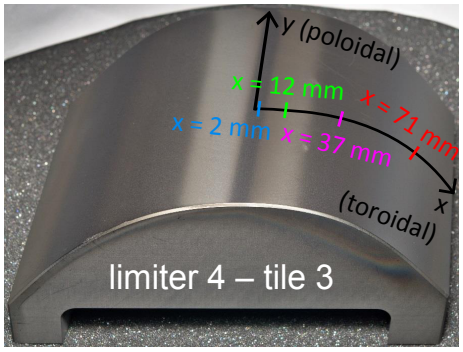

Figure 3: Photo of limiter 4 – tile 3 with lateral position x in toroidal direction. The colored positions show the center of the identified zone.

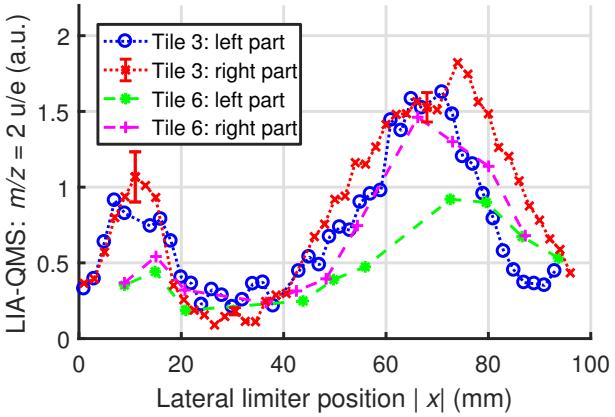

Figure 4: LIA–QMS hydrogen signals of limiter 4 – tiles 3 and 6 over toroidal direction x as surface coordinate with 0 at the center of the limiter. The signals are folded to show the symmetry for the left and right side of the limiters

Fig. 5 shows the depth resolved hydrogen signals for the local extrema of tile 3 in Fig. 4. The laser–induced ablation rate was measured ex–situ with a profilometer. The depth distribution of the hydrogen content is different in these four zones on the limiter, which is consistent to microscopy measurements in these regions [12]:

- In the limiter center ($x = 0$ mm)–almost tangential to the plasma a low hydrogen content is observed. This zone shows a smooth erosion dominated surface due to perpendicular transport of impinging ions.
- Nearby the limiter center ($x = (12 \pm 5)$ mm) a mixed zone with high hydrogen content in small depth is observed.
- Next to this area ($x = (30 \pm 10)$ mm) a small amount of hydrogen indicates a pure erosion zone where hydrogen is only implanted in the material.
- On the outer part of the limiter tile ($x = (70 \pm 20)$ mm), located deepest in the scrape–off layer, a net–deposition zone is observed: A layer of re–deposited carbon and co–deposited hydrogen

with a thickness up to 600 μm is formed during OP 1.1. The thickness is in good agreement with EDX measurements [13].

The overall erosion deposition pattern with an almost untouched top surface and strong deposition on the side areas is comparable to observation in limiter tokamaks[3, 16].

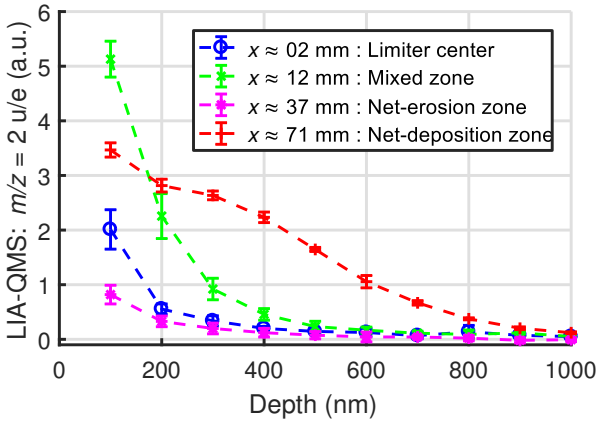

Figure 5: Depth resolved hydrogen signal for different toroidal positions x on limiter 4 – tile 3 which show zones of different plasma interaction with the surface.

4.2. Poloidal

Comparable hydrogen contents and depth distributions are found for the net–deposition zone of the right part of tile 3 and tile 6 (Fig. 4), although an asymmetry of the heat flux on the limiter tiles is observed (compare Fig. 1). For tile 6, the left part shows a 30% lower hydrogen signal in the net–deposition zone. Also the hydrogen content of tile 6 in the mixed zone is 50% lower than on tile 3.

4.3. Toroidal: tile 3 of limiter 1,2 and 4

Fig. 6 shows a comparison of limiter 1 and limiter 4 – tile 3 in toroidal direction. Within the measurement uncertainty, limiter 1 shows a similar amount of hydrogen and oxygen in the net–deposition zone, whereas the signals of limiter 1 in the mixed zone are comparatively small to the erosion dominated zone. This is attributed to the fact, that limiter 1 was exposed to up to 2 times higher heat load[11] associated with significant higher surface temperature which causes less hydrogen stored in the layer.

With deviation of the signals for limiter 2 in the four identified zone from limiter 4 being lower than $0.2 \cdot 10^{22}$hydrogen atoms/m² (not shown), the hydrogen content of these limiters are equivalent within the measurement uncertainty.

The signals in Fig. 6 were calibrated using TDS results of the deposition zone on limiter 4, which is discussed in more detail in section 4.4.

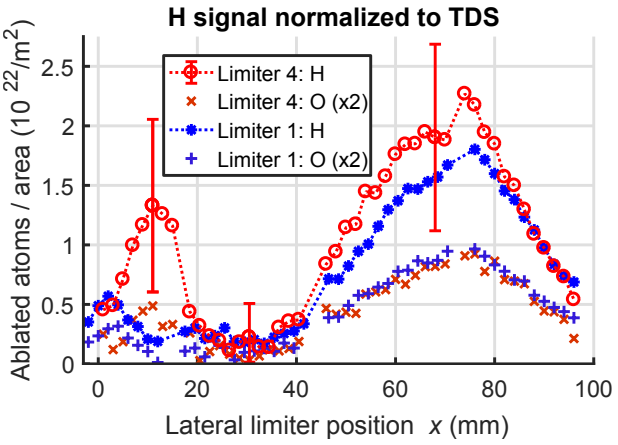

Figure 6: Comparison of the hydrogen and oxygen content of limiter tiles 3 in different modules of W7–X.

4.4. Quantification

To quantify the LIA–QMS results, two calibration procedures can be used: On the one hand, TDS measurements using small pieces of the limiter tiles was performed. On the other hand a calibration leak, which is integrated in the setup, can be used with each analyzed gas. TDS results are shown in Tab 2.

Table 2: TDS measurement results of limiter tile pieces from the identified zones and the extracted plasma–induced H content increase. Errors include uncertainties of the calibration leak and of the sample size measurements.

Sample	TDS signal (10^{18} H atoms)	Plasma–induced signal (10^{22} H atoms/m^2)
Reference	(0.80 ± 0.12)	–
Mixed	(1.79 ± 0.27)	(1.55 ± 0.60)
Net–erosion	(1.04 ± 0.16)	(0.38 ± 0.43)
Net–deposition	(2.00 ± 0.30)	(1.88 ± 0.66)

To minimize measurement uncertainties, all pieces were cut to the same dimensions. A unexposed graphite limiter tile was outgassed (*Reference sample*) to determine the hydrogen content in the graphite before plasma exposure. After subtraction of the reference's hydrogen content, the signals of pieces from the center of the identified zones were normalized to the exposed surface area. This evaluation extracts the plasma–induced hydrogen signal[2]. In the net–erosion zone, hydrogen can only be implanted, resulting in a low hydrogen TDS signal as well as LIA–QMS signal for $^m/_z = 2\,^u/_e$. For the mixed and net–deposition zone, additionally a layer of re–deposited carbon with co–deposited hydrogen and oxygen [12] results

[2]For error calculations the uncertainty of the calibration leak of 10% is used for TDS. The sample size uncertenties are $\Delta x_i = 0.1$ mm. Hydrogen contamination from the sides of the samples after cutting is neglected.

in a 4 to 5 times higher hydrogen signal. Moreover, the TDS results show ten percent lower hydrogen content in the mixed zone compared to the deposition zone, whereas the signal is about 50% lower for LIA–QMS (Fig. 4) and LIBS [13].

Using TDS as calibration for LIA–QMS requires an additional post–mortem analysis procedure with lower lateral resolution and without depth information. Another method to quantify the quadruple signal bases on a calibration leak with known flow rate: With closed shutter to the vacuum pumps, hydrogen gas is filled into the vacuum chamber with a flow rate of $\Delta QH_2 = (9.13 \pm 0.73) \cdot 10^{-7}\,\mathrm{Pa\,m^3/s}$. Using the quadrupole detector current rise and the flow rate, the detector signal can be converted to a hydrogen partial pressure and hence to an absolute number of hydrogen atoms when the ideal gas equation is applied. Details to this calibration procedure can be found in [14]. Using this calibration method, the hydrogen content is 35 % lower than for TDS in the mixed and the net–deposition zone. Potential reasons for discrepancy are: Firstly, hydrogen can be implanted deeper in the material than 1 μm, so that is not detected by LIA–QMS, but outgassed with TDS. Also the unexposed reference sample might be slightly different in its fuel content. Moreover, for picosecond laser–induced ablation, the induced plasma does not necessarily break all chemical bonds during the ablation process. Consequently, a fraction of the hydrogen remains in hydrocarbons. A composition analysis is performed by sweeping the quadrupole for $^m/_z = 2\,\mathrm{u/e} - 100\,\mathrm{u/e}$ to show the ablated hydrocarbons.

4.5. Surface composition analysis

A residual gas spectrum for the first laser–induced ablation pulse on limiter 4 – tile 3 in the net–deposition zone is shown in Fig. 7. The constant laser–induced signal after 15 laser pulses is overlayed as background signal (*BG ablation*) in white. Besides hydrogen ($^m/_z = 2\,\mathrm{u/e}$) and oxygen ($^m/_z = (32 \text{ and } 16)\,\mathrm{u/e}$), LIA–QMS analysis shows significant signals for (12–16) u/e and (25–28) u/e. A possible solution for the composition division with hydrocarbons, nitrogen and carbon monoxide is presented[3]. The C_2H_x signals for $^m/_z = (25\text{–}27)\,\mathrm{u/e}$ indicate, that after picosecond laser–induced ablation of the net–deposition layer, carbon hydirdes needs to be included for quantitative analysis using LIA–QMS. The signal of $^m/_z = 28\,\mathrm{u/e}$ is a superposition of hydrocarbons, nitrogen and carbon monoxide. As the signal of $^m/_z = 30\,\mathrm{u/e}$ is low, no significant amount of C_2H_6 seems to be ablated. A drawback of quantitative LIA–QMS analysis is, that each gas needs to be calibrated individually. Further investigations are required for a more detailed quantitative analysis of the composition division.

[3]Cracking patterns for O_2, N_2 and CH_4 were measured using gas inlet by the calibration leak. As the results are in good agreement ($\Delta I < 5\%$) with mass spectra from [17], its cracking patterns were included for C_2H_2 and C_2H_4 in Fig. 7.

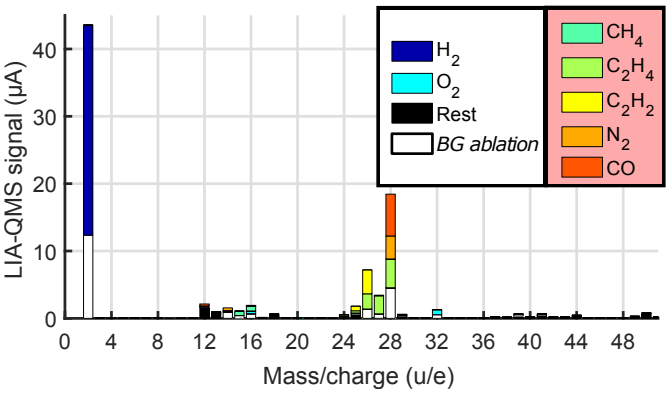

Figure 7: Possible solution for the composition division of the first laser pulse in the deposition dominated zone. Pulse number 15 in white is showing the constant background (*BG ablation*) signal. For interpretation of the references to color in this figure legend, the reader is referred to the web version of this article.

5. Conclusion

LIA–QMS results for the hydrogen content of graphite limiter tiles from W7–X OP 1.1 are in good agreement with LIBS measurements. In toroidal direction LIA–QMS analysis shows, that signals of hydrogen and oxygen close to the limiter center are lower for limiter 1 than for limiter 2 and 4. This implies that no mixed zone is present on limiter 1 as the erosion rate is higher than the deposition rate near the limiter center, caused by a two times higher heat flux on this limiter tile. In poloidal direction, no significant variation of the hydrogen content is observed for the deposition dominated zone, whereas the hydrogen content in the mixed zone of tile 6 is 50% lower than in the mixed zone of tile 3.

A composition analysis of the residual gas spectrum shows, that hydrocarbons include a significant amount of hydrogen in the residual gas spectrum. These need to be included for quantitative hydrogen content measurements using LIA–QMS analysis and and also to be considered for the interpretation of picosecond LIBS results.

Future analysis will be performed with graphite divertor tiles from OP 1.2. Furthermore, LIA–QMS technique will be improved and tested under W7–X like conditions as a possible in–situ diagnostic for hydrogen retention monitoring in fusion devices.

Acknowledgement

This work has been carried out within the framework of the EUROfusion Consortium and has received funding from the Euratom research and training programme 2014-2018 under grant agreement No 633053. The views and opinions expressed herein do not necessarily reflect those of the European Commission.

References

[1] S. Brezinsek, M. Jakubowski, Plasma-Surface Interaction and Plasma-Edge Studies in Wendelstein 7-X Operating with Passively Cooled Graphite Divertor, 45th EPS Conference on Plasma Physics, I3.111, 2018.

[2] O. Neubauer, W. Biel, et al., Diagnostic setup for investigation of plasma wall interactions at Wendelstein 7-X, Fusion Eng. Des. 96-97 (2015) 891–894. doi:10.1016/j.fusengdes.2015.06.102.
URL http://dx.doi.org/10.1016/j.fusengdes.2015.06.102

[3] A. Kirschner, V. Philipps, et al., Simulation of the plasma – wall interaction in a tokamak with the Monte Carlo code ERO-TEXTOR, Nucl. Fusion 40 (5) (2000) 989.
URL http://dx.doi.org/10.1088/0029-5515/40/5/311

[4] T. S. Pedersen, M. Otte, et al., Confirmation of the topology of the Wendelstein 7-X magnetic field to better than 1:100,000, Nat. Commun. 7 (December). doi:10.1038/ncomms13493.

[5] T. S. Pedersen, A. Dinklage, et al., Key results from the first plasma operation phase and outlook for future performance in Wendelstein 7-X, Phys. Plasmas 24 (5) (2017) 0–10. doi:10.1063/1.4983629.

[6] J. Roth, E. Tsitrone, et al., Recent analysis of key plasma wall interactions issues for ITER, J. Nucl. Mater. 390-391 (1) (2009) 1–9. doi:10.1016/j.jnucmat.2009.01.037.

[7] V. Philipps, A. Malaquias, et al., Development of laser-based techniques for in situ characterization of the first wall in ITER and future fusion devices, Nucl. Fusion 53 (9) (2013) 93002. doi:10.1088/0029-5515/53/9/093002.
URL http://stacks.iop.org/0029-5515/53/i=9/a=093002

[8] A. Malaquias, V. Philipps, et al., Development of ITER relevant laser techniques for deposited layer characterisation and tritium inventory, J. Nucl. Mater. 438 (2013) S936–S939. doi:10.1016/j.jnucmat.2013.01.203.
URL http://dx.doi.org/10.1016/j.jnucmat.2013.01.203

[9] D. W. Hahn, N. Omenetto, Laser Induced Breakdown Spectroscopy (LIBS), Part II: Review of Instrumental and Methodological Approaches to Material Analysis and Applications to Different Fields, Appl. Spectrosc. 66 (4) (2012) 347–419. doi:10.1366/11-06574.

[10] R. Fantoni, S. Almaviva, et al., Development of Calibration-Free Laser-Induced-Breakdown-Spectroscopy based techniques for deposited layers diagnostics on ITER-like tiles, Spectrochim. Acta - Part B At. Spectrosc. 87 (2013) 153–160. doi:10.1016/j.sab.2013.05.032.

[11] G. A. Wurden, C. Biedermann, et al., Limiter observations during W7-X first plasmas, Nucl. Fusion 57 (5). doi:10.1088/1741-4326/aa6609.

[12] V. R. Winters, S. Brezinsek, et al., Overview of the plasma-surface interaction on limiter surfaces in the startup campaign of Wendelstein 7-X, Phys. Scr. T170 (2017) 014050. doi:10.1088/1402-4896/aa8e21.
URL http://stacks.iop.org/1402-4896/2017/i=T170/a=014050?key=crossref.d9b163919ac7528ad1afcddb2c1b7078

[13] C. Li, N. Gierse, et al., Laser-induced breakdown spectroscopy for Wendelstein 7-X stellarator limiter tile analysis, in: Phys. Scr., no. T170, IOP Publishing, 2017. doi:10.1088/0031-8949/2017/T170/014004.

[14] J. Oelmann, N. Gierse, et al., Depth-resolved sample composition analysis using laser-induced ablation-quadrupole mass spectrometry and laser-induced breakdown spectroscopy, Spectrochim. Acta - Part B At. Spectrosc. 144 (2018) 38–45. doi:10.1016/j.sab.2018.03.009.

[15] R. C. Wolf, A. Ali, et al., Major results from the first plasma campaign of the Wendelstein 7-X stellarator, Nucl. Fusion 57 (10) (2017) 102020.

[16] S. Brezinsek, A. Pospieszczyk, et al., Hydrocarbon injection for quantification of chemical erosion yields in tokamaks, J. Nucl. Mater. 363-365 (1-3) (2007) 1119–1128. doi:10.1016/j.jnucmat.2007.01.190.

[17] P. J. Linstrom, W. G. Mallard (Eds.), NIST Chemistry WebBook, NIST Standard Reference Database Number 69, National Institute of Standards and Technology, Gaithersburg MD, 20899, 2005.
URL http://webbook.nist.gov